Jurnal
Teknologi

Full Paper

THE VISCOUS DISSIPATION EFFECTS ON THE MIXED CONVECTION BOUNDARY LAYER FLOW ON A HORIZONTAL CIRCULAR CYLINDER

Muhammad Khairul Anuar Mohamed[a], Mohd Zuki Salleh[a]*, Nor Aida Zuraimi Md Noar[a], Anuar Ishak[b]

[a]Applied & Industrial Mathematics Research Group, Fakulti Sains & Teknologi Industri, Universiti Malaysia Pahang, 26300 UMP Kuantan, Pahang, Malaysia
[b]Pusat Pengajian Sains Matematik, Fakulti Sains & Teknologi, Universiti Kebangsaan Malaysia, 43600 UKM Bangi, Selangor, Malaysia

Article history
Received
25 October 2015
Received in revised form
14 December 2015
Accepted
9 February 2016

*Corresponding author
zukikuj@yahoo.com

Graphical abstract

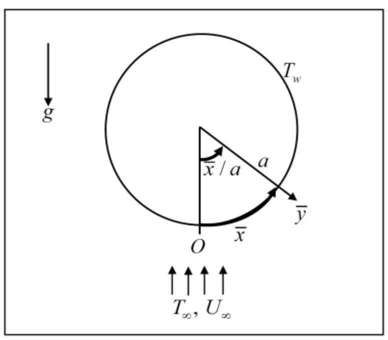

Abstract

Present study consider the mathematical modeling for mixed convection boundary layer flow and heat transfer on a horizontal circular cylinder with viscous dissipation. The transformed partial differential equations are solved numerically by using an implicit finite-difference scheme known as the Keller-box method. Numerical solutions are obtained for the reduced Nusselt number, the local skin friction coefficient, the velocity and temperature profiles. The features of the flow for various values of the Prandtl number, Eckert number and mixed convection parameter are discussed. The results in this paper is original and important for the researchers working in the area of boundary layer flow and this can be used as reference and also as complement comparison purpose in future.

Keywords: Mixed convection, horizontal circular cylinder, viscous dissipation

1.0 INTRODUCTION

Mixed convection actually is the combination of the free and the forced convection where mixed convection parameter λ take part as scalar to measure the influence of free and forced convection in a flow. Accordings to Pop and Ingham [1] and Kreith et al. [2], the forced convection is dominant when $\lambda \to 0$, while free convection take part as $\lambda \to \infty$. The application of mixed convection are widely used in engineering and industrial outputs for an example in engine and transmission cooling system such as cooling fins in car radiator, nuclear reactant power plant, air conditioner, refrigerator and many more. The geometry of the surface that are commonly used and studied by the researchers such as the cylinder surface, solid sphere, cone, stagnation region and stretching plate.

It is known that the momentum equation of forced convection boundary layer flow is first solved by Blasius [3]. The energy equation for this problem then solved by Frössling [4]. It is worth to mention that, the constant wall temperature (CWT) is considered. Gebhart and Pera [5] done the experimental studies on long horizontal cylinders. The heat transfer of mixed convection on several type of fluid on various lengths of wires are reported. Merkin [6] solved the governing equations for the model of mixed convection on horizontal circular cylinder. The solution is obtained for $\mathrm{Pr}=1$ and it is found that there exist a separation where there is no solution or the boundary layer equation are not valid after the separation point. Jain and Lohar [7] considered the unsteady case for this topic. The variations of mean Nusselt number with time are shown and discussed. Next, Nazar et al. [8] extended the works by Merkin [6] with micropolar fluid while Anwar et al. [9] considered viscoelastic fluid. Both problems are solved by using the Keller-box method. The point of separation for the boundary layer, effects of Prandtl number and mixed convection parameter are discussed in detail. Further, Salleh et al. [10] investigated this topic by considering the Newtonian heating as a boundary conditions. Other researchers who considered this topic including Ahmad et al. [11], Rahman et al. [12], Nazar et al. [13], Rashad et al. [14] and recently by Tham et al. [15] who investigated the nanofluid as a convective medium with porous effects. The mathematical nanofluid model is analyzed based on the Buongiorno–Darcy model.

In all investigations above, the viscous dissipations is neglected. According to Gebhart [16], the viscous dissipation are appreciable when the induced kinetic energy becomes significant compared to the amount of heat transferred. In other words, the viscous dissipation or internal friction is the rate of the work done againts viscous forces is irreversibly converted into internal energy. It is known that the effects of viscous dissipation is significant especially for high velocity flow, highly viscous flow with moderate velocity and for fluid with moderate Prandtl number and velocities. The characterictics of the viscous dissipation are commonly represent by Eckert number which usually denoted as Ec.

Motivated from the above-mentioned and literature studies, this topic is important and interesting to be study. Further, the authors confident that the results reported here are new.

2.0 MATHEMATICAL FORMULATION

It is consider the horizontal circular cylinder with radius a, which is heated to a constant temperature T_w embedded in an incompressible viscous fluid with ambient temperature T_∞. The orthogonal coordinates of $\bar{x}$ and $\bar{y}$ are measured along the cylinder surface, starting at the lower stagnation point $\bar{x}=0$, and normal to it, respectively. The physical model of the coordinate system are shown in Figure 1.

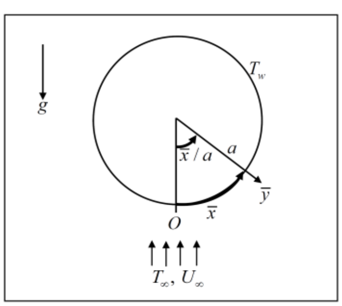

Figure 1 Physical model of the coordinate system

Under the assumptions that the boundary layer approximations is valid, the dimensional governing equations of steady mixed free convection boundary layer flow are ([6], [8], [10]):

$$\frac{\partial \bar{u}}{\partial \bar{x}}+\frac{\partial \bar{v}}{\partial \bar{y}}=0, \tag{1}$$

$$\bar{u}\frac{\partial \bar{u}}{\partial \bar{x}}+\bar{v}\frac{\partial \bar{u}}{\partial \bar{y}}=\bar{u}_e\frac{d\bar{u}_e}{d\bar{x}}+\nu\frac{\partial^2 \bar{u}}{\partial \bar{y}^2}\pm g\beta(T-T_\infty)\sin\frac{\bar{x}}{a}, \tag{2}$$

$$\bar{u}\frac{\partial T}{\partial \bar{x}}+\bar{v}\frac{\partial T}{\partial \bar{y}}=\alpha\frac{\partial^2 T}{\partial \bar{y}^2}+\frac{\mu}{\rho C_p}\left(\frac{\partial \bar{u}}{\partial \bar{y}}\right)^2, \tag{3}$$

with the boundary conditions

$$\bar{u}(\bar{x},0)=\bar{v}(\bar{x},0)=0,\ T(\bar{x},0)=T_w, \\ \bar{u}(\bar{x},\infty)\to\bar{u}_e,\ T(\bar{x},\infty)\to T_\infty \tag{4}$$

where $\bar{u}$ and $\bar{v}$ are the velocity components along the $\bar{x}$ and $\bar{y}$ axes, respectively. μ is the dynamic viscosity, g is the gravity acceleration, ν is the kinematic viscosity, α is the thermal diffusivity, β is the thermal expansion, T is the local temperature, ρ is the fluid density and C_p is the specific heat capacity at a constant pressure. Further, $\bar{u}_e(x)$ is given by

$$\bar{u}_e(x)=U_\infty\sin\left(\frac{\bar{x}}{a}\right). \tag{5}$$

Next, it is introduced the governing non-dimensional variables:

$$x=\frac{\bar{x}}{a},\quad y=\mathrm{Re}_x^{1/2}\frac{\bar{y}}{a},\quad u=\frac{\bar{u}}{U_\infty}, \\ v=\mathrm{Re}_x^{1/2}\frac{\bar{v}}{U_\infty},\quad \theta(\eta)=\frac{T-T_\infty}{T_w-T_\infty},\quad u_e(x)=\frac{\bar{u}_e(x)}{U_\infty}. \tag{6}$$

Using variables (6), equations (1) to (3) becomes

$$\frac{\partial u}{\partial x}+\frac{\partial v}{\partial y}=0, \tag{7}$$

$$u\frac{\partial u}{\partial x}+v\frac{\partial u}{\partial y}=u_e\frac{du_e}{dx}+\frac{\partial^2 u}{\partial y^2}+\lambda\theta\sin x, \tag{8}$$

$$u\frac{\partial \theta}{\partial x}+v\frac{\partial \theta}{\partial y}=\frac{1}{\mathrm{Pr}}\frac{\partial^2\theta}{\partial y^2}+Ec\left(\frac{\partial u}{\partial y}\right)^2, \tag{9}$$

and the boundary conditions (4) become

$$u(x,0)=0,\ v(x,0)=0,\ \theta(x,0)=1, \\ u(x,\infty)\to u_e,\ \theta(x,\infty)\to 0 \tag{10}$$

where $Ec = \dfrac{U_\infty{}^2}{C_p\left(T_w - T_\infty\right)}$ is an Eckert number and $\Pr = \dfrac{\nu}{\alpha}$ is the Prandtl number. Note that λ is the mixed convection parameter which is given by $\lambda = \dfrac{Gr}{\mathrm{Re}_x^2}$ where $\mathrm{Re} = \dfrac{U_\infty a}{\nu}$ is the Reynolds number and $Gr = \dfrac{g\beta(T_w - T_\infty)a^3}{\nu^2}$ is the the Grashof number.

In order to solve equations (7) to (9), the following function is introduced:

$$\psi = xf(x,y), \qquad \theta = \theta(x,y), \tag{11}$$

where ψ is the stream function defined as $u = \dfrac{\partial\psi}{\partial y}$ and $v = -\dfrac{\partial\psi}{\partial x}$ which identically satisfies (6) and θ is the rescaled dimensionless temperature of the fluid. Substitute (11) into (7) to (9), then the following partial differential equations is obtained:

$$\frac{\partial^3 f}{\partial y^3} + f\frac{\partial^2 f}{\partial y^2} - \left(\frac{\partial f}{\partial y}\right)^2 + \frac{\sin x}{x}\left(\lambda\theta + \cos x\right) = x\left(\frac{\partial f}{\partial y}\frac{\partial^2 f}{\partial x \partial y} - \frac{\partial f}{\partial x}\frac{\partial^2 f}{\partial y^2}\right), \tag{12}$$

$$\frac{1}{\Pr}\frac{\partial^2\theta}{\partial y^2} + f\frac{\partial\theta}{\partial y} = x\left(\frac{\partial f}{\partial y}\frac{\partial\theta}{\partial x} - \frac{\partial f}{\partial x}\frac{\partial\theta}{\partial y} - xEc\left(\frac{\partial^2 f}{\partial y^2}\right)^2\right), \tag{13}$$

the boundary conditions (10) become

$$f(x,0) = 0, \quad \frac{\partial f}{\partial y}(x,0) = 0, \quad \theta(x,0) = 1, \qquad \frac{\partial f}{\partial y}(x,\infty) \to \frac{\sin x}{x}, \quad \theta(x,\infty) \to 0 \tag{14}$$

The physical quantities of interest are the local skin friction coefficient C_f and the local Nusselt number Nu_x are:

$$C_f = \frac{\tau_w}{\rho U_\infty^2}, \qquad Nu_x = \frac{aq_w}{k(T_w - T_\infty)}. \tag{15}$$

The surface shear stress τ_w and the surface heat flux q_w are given by

$$\tau_w = \mu\left(\frac{\partial \bar{u}}{\partial \bar{y}}\right)_{\bar{y}=0}, \qquad q_w = -k\left(\frac{\partial T}{\partial \bar{y}}\right)_{\bar{y}=0}, \tag{16}$$

with $\mu = \rho\nu$ and k being the dynamic viscosity and the thermal conductivity, respectively. Using (6) and (11) give

$$C_f\,\mathrm{Re}_x^{1/2} = \left(x\frac{\partial^2 f}{\partial y^2}\right)_{\bar{y}=0} \quad \text{and} \quad Nu_x\,\mathrm{Re}_x^{1/2} = -\left(\frac{\partial\theta}{\partial y}\right)_{\bar{y}=0}. \tag{17}$$

Furthermore, the velocity profiles and temperature distributions can be obtained from the following relations:

$$u = f'(x,y), \qquad \theta = \theta(x,y), \tag{18}$$

two-component gel, it is easy to modify the molecular structure of either of the two components.

3.0 RESULTS AND DISCUSSION

Equations (12) and (13) with (14) were solved numerically using the finite different scheme method known as Keller-box method. Three parameters are considered, namely the Prandtl number $\Pr$, Eckert number Ec and the mixed convection parameter λ. In order to solve this problem, the step size $\Delta y = 0.02, \Delta x = 0.01$ and boundary layer thickness $y_\infty = 8$ and $x_\infty = \pi$ are used. Table 1 shows the comparison values of $Nu_x\,\mathrm{Re}_x^{-1/2}$ with previous results by Merkin [6] and Nazar [17] when the viscous dissipation effects is neglected $(Ec = 0)$. It is concluded that the Keller-box method is efficiently and very accurate to solve this problems since the results is in a good agreement.

Table 1 Comparison values of $Nu_x \mathrm{Re}_x^{-1/2}$ with previous published results for different values of x and λ when $\mathrm{Pr}=1, Ec=0.$

x/λ	-1.0			0			1.0		
	Nazar [17]	Merkin [6]	Present	Nazar [17]	Merkin [6]	Present	Nazar [17]	Merkin [6]	Present
0	0.5080	0.5067	0.5067	0.5710	0.5705	0.5705	0.6160	0.6156	0.6156
0.2	0.5022	0.5018	0.5016	0.5658	0.5658	0.5669	0.6125	0.6115	0.6126
0.4	0.4862	0.4865	0.4862	0.5560	0.5564	0.5564	0.6031	0.6028	0.6037
0.6	0.4584	0.4594	0.4589	0.5380	0.5391	0.5389	0.5880	0.5885	0.5892
0.8	0.4140	0.4160	0.4151	0.5130	0.5145	0.5143	0.5673	0.5686	0.5690
1.0	0.3259	0.3326	0.3301	0.4808	0.4826	0.4823	0.5414	0.5435	0.5436
1.2				0.4406	0.4426	0.4414	0.5105	0.5133	0.5126
1.4				0.3909	0.3928	0.3912	0.4750	0.4785	0.4774
1.6				0.3262	0.3280	0.3258	0.4354	0.4394	0.4381
1.8				0.2049	0.2114	0.2043	0.3924	0.3967	0.3951
2.0							0.3465	0.3509	0.3500
2.2							0.3002	0.3029	0.3013
2.4							0.2515	0.2540	0.2526
2.6							0.2040	0.2061	0.2051
2.8							0.1636	0.1634	0.1632
3.0							0.1397	0.1354	0.1371
π							0.1380	0.1306	0.1327

Tables 2 and 3 present the values of $Nu_x \mathrm{Re}_x^{-1/2}$ and $C_f \mathrm{Re}_x^{1/2}$ with different values of x and λ. From Table 2, it is found that the increase of x results to the decrease of $Nu_x \mathrm{Re}_x^{-1/2}$. Physically, it is means that there is reducing in convective heat transfer capabilities. From Table 3, $C_f \mathrm{Re}_x^{1/2}$ increase from the stagnation region $(x=0)$ to the middle of cylinder before decrease back until at the end of the cylinder $(x=\pi)$. As tables goes to the right, both values of $Nu_x \mathrm{Re}_x^{-1/2}$ and $C_f \mathrm{Re}_x^{1/2}$ increase with λ. From numerical results, it is found that the increase of λ delays separation. From these tables, the $\lambda \geq 1$ gives no separation and according to Merkin [6] and Nazar [17], the value of λ which first gives no separation for this viscous fluid lies between $0.88 \leq \lambda \leq 0.89.$

Figures 2 and 3 displayed the temperature profiles for different values of Pr and λ, respectively. It is found that the increase of Pr or λ have reduce its thermal boundary layer thickness. It is due to decrease in thermal diffusivity which reduced the energy ability and the thermal boundary layer thickness.

Next, Figure 4 shows the variations of $Nu_x \mathrm{Re}_x^{-1/2}$ with different values of Ec against x. It is seen that the viscous dissipation Ec are negligible at the lower stagnation region $(x=0)$. The effects of Ec are significance as x increase to the middle of cylinder then converged back at the end of the cylinder $(x=\pi)$.

Table 2 Values of $Nu_x \mathrm{Re}_x^{-1/2}$ with different values of x and λ when $\mathrm{Pr}=1, Ec=0.1.$

x/λ	-1.0	-0.5	0	0.5	1.0	2.0
0	0.5067	0.5421	0.5705	0.5945	0.6156	0.6515
0.2	0.5004	0.5364	0.5648	0.5887	0.6094	0.6444
0.4	0.4821	0.5202	0.5490	0.5723	0.5932	0.6246
0.6	0.4513	0.4944	0.5241	0.5470	0.5655	0.5940
0.8	0.4045	0.4598	0.4921	0.5148	0.5320	0.5558
1.0	0.3158	0.4162	0.4545	0.4782	0.4943	0.5134
1.2		0.3592	0.4122	0.4391	0.4551	0.4699
1.4		0.2533	0.3641	0.3985	0.4161	0.4282
1.6			0.3048	0.3564	0.3782	0.3899
1.8			0.1939	0.3112	0.3413	0.3558
2.0				0.2589	0.3048	0.3255
2.2					0.2678	0.2984
2.4					0.2297	0.2734
2.6					0.1914	0.2498
2.8					0.1562	0.2268
3.0					0.1330	0.2031
π					0.1289	0.1847

Table 3 Values of $C_f \mathrm{Re}_x^{1/2}$ with different values of x and λ when $\Pr = 1$, $Ec = 0.1$.

x/λ	-1.0	-0.5	0	0.5	1.0	2.0
0	0	0	0	0	0	0
0.2	0.1254	0.1868	0.2425	0.2943	0.3433	0.4350
0.4	0.2253	0.3501	0.4619	0.5655	0.6612	0.8459
0.6	0.2753	0.4684	0.6376	0.7936	0.9388	1.2104
0.8	0.2491	0.5232	0.7524	0.9598	1.1529	1.5110
1.0	0.0906	0.4991	0.7943	1.0541	1.2935	1.7336
1.2		0.3798	0.7563	1.0706	1.3548	1.8714
1.4		0.1047	0.6366	1.0100	1.3377	1.9234
1.6			0.4328	0.8797	1.2555	1.8951
1.8			0.0921	0.6916	1.1039	1.7975
2.0				0.4598	0.9186	1.6457
2.2					0.7147	1.4570
2.4					0.5146	1.2485
2.6					0.3400	1.0347
2.8					0.2107	0.8344
3.0					0.1428	0.6159
π					0.1333	0.4645

Figures 5 and 6 are plotted in order to understand the behavior of $C_f \mathrm{Re}_x^{1/2}$ for both parameter Ec and λ, respectively. In Figure 5, at the early stage, it is found that the $C_f \mathrm{Re}_x^{1/2}$ is unique for all Ec value. From figure, it is understand that the Ec influenced a small effects on $C_f \mathrm{Re}_x^{1/2}$. Noticed that as Ec increases, the $C_f \mathrm{Re}_x^{1/2}$ also increases. In Figure 6, the effect of mixed convection parameter λ is large on $C_f \mathrm{Re}_x^{1/2}$ where increases as $C_f \mathrm{Re}_x^{1/2}$ as λ increases. It is also clearly seen the variation of the separation point for λ and the $C_f \mathrm{Re}_x^{1/2}$ achieved its maximum value at the middle of the curve.

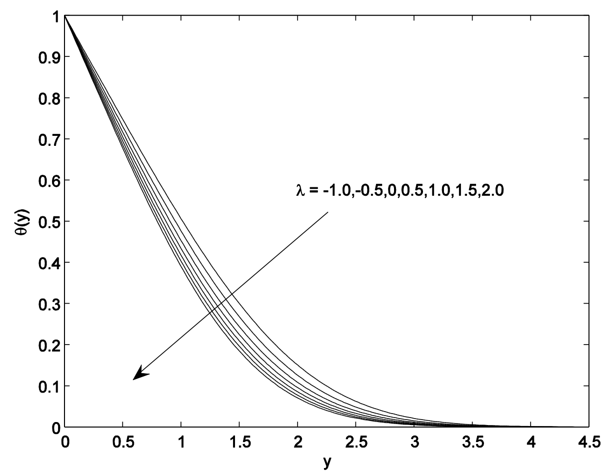

Figure 3 Temperature profiles $\theta(y)$ against y for different values of λ.

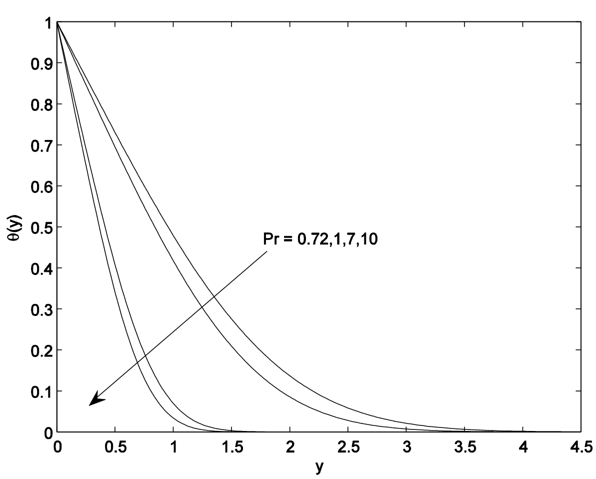

Figure 2 Temperature profiles $\theta(y)$ against y for different values of $\Pr$.

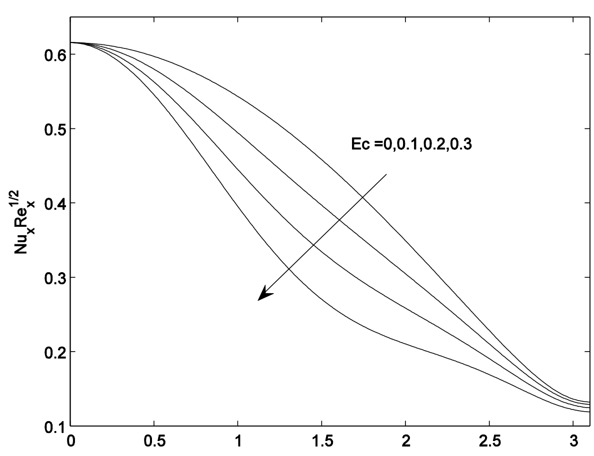

Figure 4 Reduced Nusselt number $Nu_x \mathrm{Re}_x^{-1/2}$ against x for different values of Ec.

Lastly, Figure 7 presents the velocity profiles $f'(y)$ for different values of λ. It is found that the boundary layer thickness decreases as λ increases. But this situation is valid for $\lambda < 1$. The situation is opposite for $\lambda > 1$ whereas the boundary layer thickness increase as λ increase.

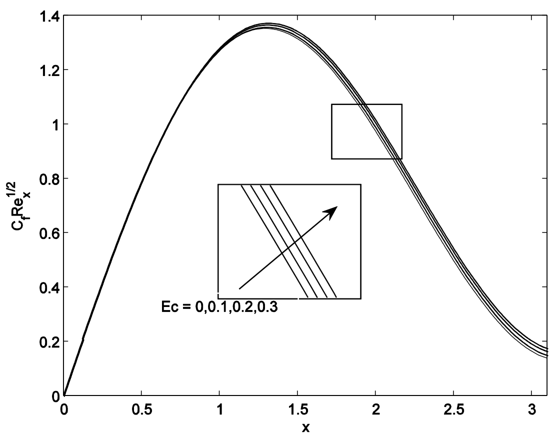

Figure 5 Reduced Skin friction coefficient $C_f \mathrm{Re}_x^{1/2}$ against x for different values of Ec.

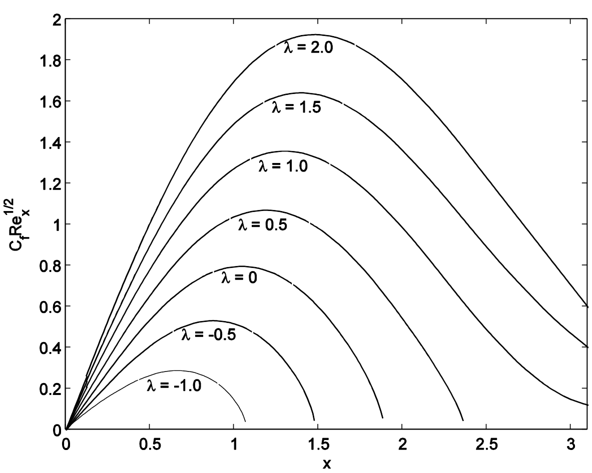

Figure 6 Reduced Skin friction coefficient $C_f \mathrm{Re}_x^{1/2}$ against x for different values of λ.

4.0 CONCLUSION

In this paper, the mathematical modeling of mixed convection boundary layer flow on horizontal circular cylinder with viscous dissipation have been solve numerically. It is shown how the Prandtl number Pr, Eckert number Ec and the mixed convection parameter λ affect the values of the reduced Nusselt number and reduced skin friction coefficient as well as the velocity and temperature profiles.

As a conclusion, the increase of Pr result to the decrease of thermal boundary layer thickness. It is because, an increase of Pr means the increase in viscosity but decrease in thermal diffusivity which reduced the energy ability and the thermal boundary layer thickness. Next, it is found that the increase of λ affect the increasing in reduced Nusselt number and reduced skin friction coefficient. Note that the flow separation also delayed by the increase of λ.

Next, the influenced of Ec on reduced Nusselt number are negligible at the lower stagnation region $(x = 0)$, Ec reduced Nusselt number pronouncedly at the middle of the cylinder. Meanwhile, the Ec effects are small on reduced skin friction coefficient. Lastly, it is seen that the reduced Nusselt number decreasing across the cylinder while the value of skin friction achieved its maximum value at the middle of cylinder before decreasing back at the end of cylinder $(x = \pi)$.

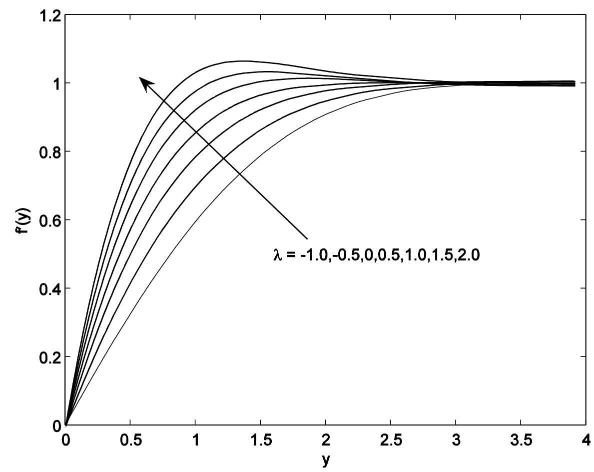

Figure 7 Velocity profiles $f'(y)$ against y for different values of λ.

Acknowledgement

The authors thank University Malaysia Pahang for the financial supports with code number RDU140111 (FRGS) and RDU150101 (FRGS).

References

[1] Pop, I. & Ingham, D. B. 2001. *Convective Heat Transfer: Mathematical and Computational Modelling of Viscous Fluids and Porous Medium.* Oxford: Pergamon.

[2] Kreith, F., Manglik, R. M. & Bohn, M. S. 2010. *Principles of Heat Transfer.* Stamford USA: Cengage Learning.

[3] Blasius, H. (1908). Boundary Layer in Fluid, Fluids with Less Friction. Z Math. Phys, 56: 1-37

[4] Frossling, N. (1958). Calculation by series expansion of the heat transfer in laminar, constant-property boundary layers at nonisothermal surfaces. Arkiv Fysik, 14:143-151

[5] Gebhart, B. & Pera, L. 1971. Mixed Convection From Long Horizontal Cylinders. *Journal of Fluid Mechanics*. 45(01): 49-64.

[6] Merkin, J. H. 1977. Mixed Convection From A Horizontal Circular Cylinder. *International Journal of Heat and Mass Transfer*. 20(1): 73-77.

[7] Jain, P. & Lohar, B. 1979. Unsteady Mixed Convection Heat Transfer From A Horizontal Circular Cylinder. *J. Heat Transfer*. 101(1): 126-131.

[8] Nazar, R., Amin, N. & Pop, I. 2003. Mixed Convection Boundary-Layer Flow From A Horizontal Circular Cylinder In Micropolar Fluids: Case Of Constant Wall Temperature. *International Journal of Numerical Methods for Heat & Fluid Flow*. 13(1): 86-109.

[9] Anwar, I., Amin, N. & Pop, I. 2008. Mixed Convection Boundary Layer Flow Of A Viscoelastic Fluid Over A Horizontal Circular Cylinder. *International Journal of Non-Linear Mechanics*. 43(9): 814-821.

[10] Salleh, M., Nazar, R. & Pop, I. 2010. Mixed Convection Boundary Layer Flow Over A Horizontal Circular Cylinder With Newtonian Heating. *Heat and Mass transfer*. 46(11-12): 1411-1418.

[11] Ahmad, S., Arifin, N. M., Nazar, R. & Pop, I. 2009. Mixed Convection Boundary Layer Flow Past An Isothermal Horizontal Circular Cylinder With Temperature-Dependent Viscosity. *International Journal of Thermal Sciences*. 48(10): 1943-1948.

[12] Rahman, M. M., Alim, M. A. & Chowdhury, M. K. 2009. *Magnetohydrodynamics Mixed Convection Around a Heat Conducting Horizontal Circular Cylinder in a Rectangular Lid-driven Cavity with Joule Heating.*

[13] Nazar, R., Tham, L., Pop, I. & Ingham, D. 2011. Mixed Convection Boundary Layer Flow From A Horizontal Circular Cylinder Embedded In A Porous Medium Filled With A Nanofluid. *Transport in porous media*. 86(2): 517-536.

[14] Rashad, A. M., Chamkha, A. J. & Modather, M. 2013. Mixed Convection Boundary-Layer Flow Past A Horizontal Circular Cylinder Embedded In A Porous Medium Filled With A Nanofluid Under Convective Boundary Condition. *Computers & Fluids*. 86(0): 380-388.

[15] Tham, L., Nazar, R. & Pop, I. 2014. Mixed Convection Flow From A Horizontal Circular Cylinder Embedded In A Porous Medium Filled By A Nanofluid: Buongiorno–Darcy Model. *International Journal of Thermal Sciences*. 84: 21-33.

[16] Gebhart, B. 1962. Effects Of Viscous Dissipation In Natural Convection. *Journal of Fluid Mechanics*. 14(02): 225-232.

[17] Nazar, R. M., "Mathematical Model for Free and Mixed Convection Boundary Layer Flows of Micropolar Fluids", PhD Thesis, Universiti Teknologi Malaysia, 2003

.